Proc Indian Natn Sci Acad **79** No. 4 December 2013 Spl. Issue, Part A, pp. 807-815

DOI: 10.16943/ptinsa/2013/v79i4/48005

Research Paper

Stability of a Long Unsupported Circular Tunnel in Clayey Soil by Using Upper Bound Finite Element Limit Analysis

J P SAHOO and J KUMAR[1,2*]
[1,2]*Department of Civil Engineering, Indian Institute of Science, Bangalore 560 012, India*

(Received 01 March 2013; Accepted 17 April 2013)

With the application of the upper bound finite element limit analysis in combination with linear optimization, the stability of a long unsupported circular tunnel (opening) in a clayey soil has been assessed. The undrained condition and the increase of cohesion of the soil mass with depth have been taken into account. The stability of the tunnel has been evaluated in the form of a non-dimensional stability number ($\gamma_{max}H/c$); where H is tunnel cover, c refers to soil cohesion, and γ_{max} is maximum unit weight of soil mass which the tunnel can support without any collapse. The variation of the stability number with H/D has been established for different values of m; where D refers to the diameter of the tunnel and m accounts for the rate at which the cohesion increases linearly with depth. The stability number increases continuously with an increase in the values of both H/D and m.

Key Words: Upper bound; Finite elements; Limit analysis; Optimization; Plasticity; Stability; Tunnel

1. Introduction

For developing better transporting facilities and to avoid congestion in traffic, underground openings/ tunnels are constructed in large cities. In order to assess the stability of tunnels and underground openings, a number of research investigations have been performed by several researchers [1-9]. Atkinson and Potts [1] have studied theoretically and experimentally the stability of supported circular tunnels in cohesionless soil. Davis *et al.* [2] obtained the solutions for evaluating the collapse of an underground opening formed in homogenous soft clay with the usage of the theorems of the limit analysis. Leca and Dormieux [3] examined the stability of shallow circular tunnels in a frictional material by employing upper and lower bound limit analysis. With the help of finite elements and linear programming, Sloan and Assadi [4] obtained rigorous bound solutions for finding the stability of a square tunnel in clay whose cohesion increases linearly with depth under undrained condition. Wu and Lee [5] carried out centrifuge model tests for single and parallel tunnels in clay to study the ground movements and the associated collapse mechanisms. Osman *et al.* [6] have developed upper bound solutions for obtaining the stability of a circular tunnel in clay based on an assumed collapse mechanism, that is, within the boundary of the deformation mechanism, the soil was assume to deform compatibly following a Gaussian distribution and outside this mechanism, the soil was assumed to be rigid. By applying the upper bound finite element limit analysis with linear programming and rigid block failure mechanism, Yang and Yang [7] calculated the internal pressure needed on the sides of rectangular shallow tunnel to maintain stability in cohesive-frictional soil. Yamamoto *et al.* [8-9] have generated stability charts for circular and square tunnels in cohesive frictional soil with the usage of the finite element limit analysis in conjunction with nonlinear programming. In the present study, a rigorous upper bound finite elements limit analysis has been

[2]**Authors for Correspondence: E-mail:jkumar@civil.iisc.ernet.in; jagdish@civil.iisc.ernet.in*

performed to assess the stability of a long unsupported circular tunnel in clay whose undrained shear strength increases linearly with depth. The failure patterns for a few cases have also been studied. To validate the present numerical computations, the results obtained from the analysis were compared with that reported in literature.

It needs to be mentioned that on the basis of the upper bound theorem of limit analysis, by satisfying given velocity boundary conditions, the magnitude of the collapse load can be simply determined by equating the rate of total work done by the external and body forces to the rate of dissipation of total internal energy. The magnitude of the collapse load determined on this basis is either greater or equal to the magnitude of the true collapse load for a material which follows an associated flow rule.

By using the limit analysis and assuming a suitable collapse mechanism, a number of investigations have been carried out by different researchers [10-15] to solve various geotechnical stability problems. However, the application of the limit analysis, with an assumption of the collapse mechanism, becomes limited to solve only simple problems, and moreover, the accuracy of the results depends on the assumptions involved in defining the failure mechanism. To overcome these limitations, more robust numerical formulations were developed by using finite elements and mathematical programming while implementing the limit analysis.

The advantage of using a numerical formulation for the bound theorems is that it can handle complex loading, complicated geometries and a variety of material failure conditions. Further, there is no need to assume any collapse mechanism in such a numerical technique. Robust numerical formulations have been developed by using finite elements and mathematical programming while employing the upper bound limit analysis [16-19]. The approach followed in this paper is that introduced by Sloan and Kleeman [18] on the basis of upper bound finite elements limit analysis and linear optimization.

2. Problem Definition and Problem Domain

A circular tunnel (opening) of diameter D is formed in a purely cohesive soil as shown in Fig. 1(a). The ground surface above the tunnel is assumed to be horizontal. The length of tunnel is very long as compared to its diameter so that the solution can be established with the help of a simple plane strain analysis. It is known that for saturated normally consolidated and lightly over consolidated clays, the cohesion of soil mass under undrained condition increases almost linearly with depth [20]. Therefore, in the case of a purely cohesive soil without any internal friction ($\phi = 0$), the cohesion of soil mass has been assumed to increase linearly with depth, and is defined by the following expression:

$$c = c_o\left(1 + m\frac{h}{D}\right) \tag{1}$$

where (i) c and c_o are the values of soil cohesion at a depth h and along ground surface, respectively, and (ii) m is a non-dimensional factor which defines the rate at which the cohesion increases with depth.

It has been assumed that no surcharge pressure acts over the ground surface. The stability of the tunnel needs to be determined by means of a dimensionless stability number (S_n)

$$S_n = \frac{\gamma_{\max} H}{c_0} \tag{2}$$

In the above expression, γ_{max} is the maximum unit weight of soil mass which can be permitted by the circular unsupported opening/tunnel for a given H/D without any collapse. The soil mass is assumed to be perfectly plastic, and it obeys Mohr-Coulomb failure criterion, and an associated flow rule.

Due to the symmetry about the vertical plane (OY), passing through the centre line of the tunnel, only one half of the total domain, as illustrated in Fig. 1(b), was chosen and its vertical and horizontal boundaries (CX and OX) were kept at sufficient distances away from the perimeter of the tunnel. The locations of these boundaries with $L = 2D - 8D$ and $d = 1D - 3D$, are found to be generally sufficient; the

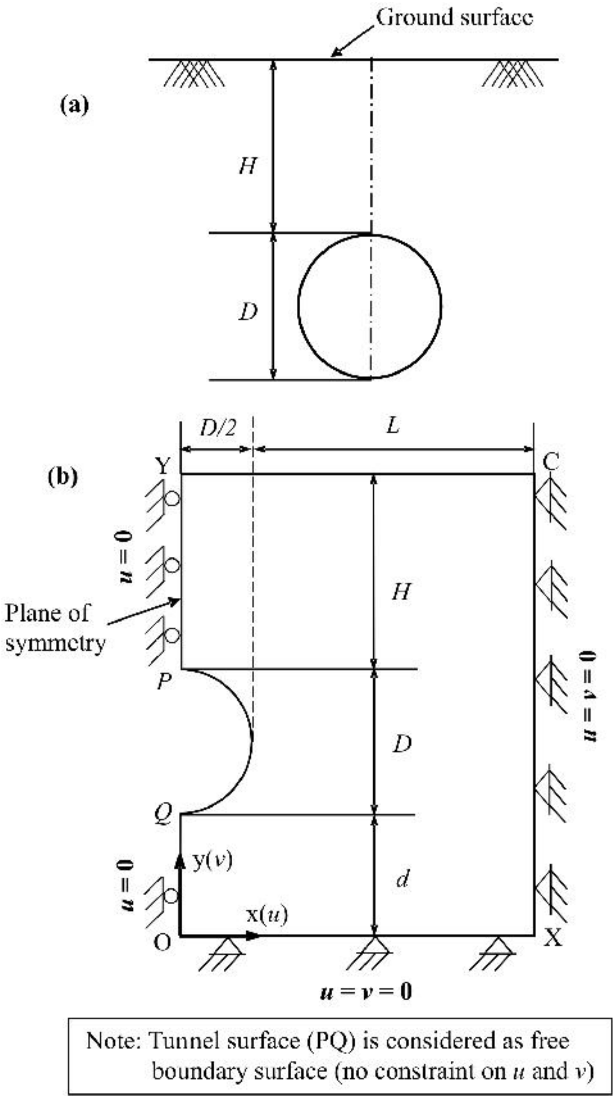

Fig. 1. (a) Definition of the problem; (b) chosen domain and associated boundary conditions

parameters L and d are defined in Fig. 1(b). The values of L and d are fixed in a way such that (i) the regions of the significant velocities are contained well within the chosen domain, and (ii) a further increase in L and d hardly causes any change in the value of the stability number.

3. Finite Element Meshes and Boundary Conditions

The chosen domain was discretized into a number of three-noded triangular elements. The sizes of the elements are gradually made smaller approaching the periphery of the tunnel. Each node remains unique to a particular element, and an interface between any two adjacent elements becomes always the line of the velocity discontinuity. The chosen finite element meshes for two different values of *H/D*, namely, 2 and 4 are illustrated in Figs. 2(a) and 2(b); in these figures, the parameters, E, N, and D_c refer to the total number of (i) elements, (ii) nodes, and (iii) discontinuities, respectively. Note that a larger size of the problem domain needs to be chosen for greater values of *H/D*: the larger size of the domain is associated with greater number of nodes, elements and velocity discontinuities. All the meshes were generated by writing the necessary preprocessing code in MATLAB. Within a given element, a linear variation of the velocities has been chosen with the application of linear shape functions. At each point

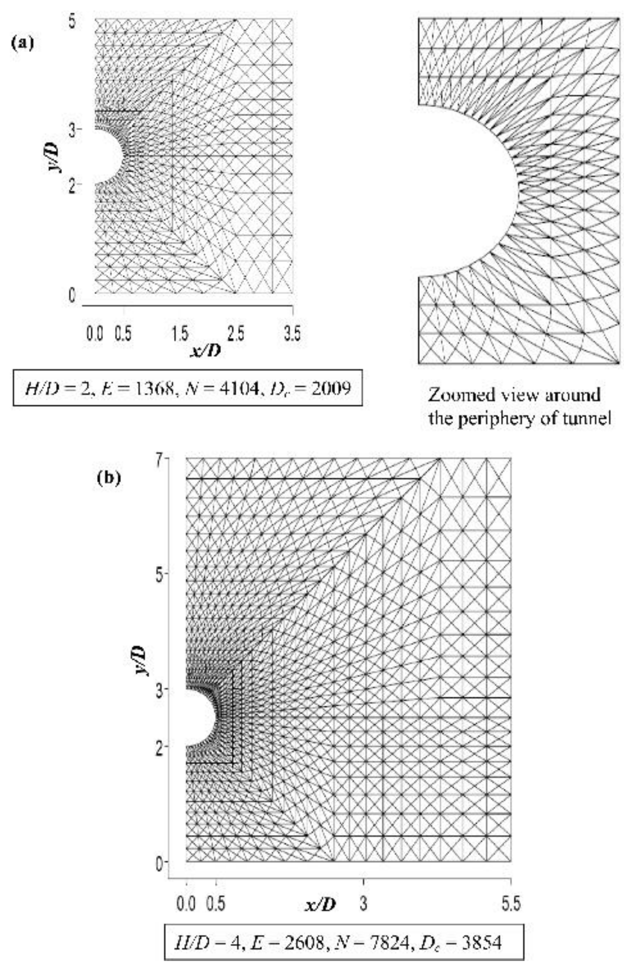

Fig. 2. The chosen finite element meshes for (a) *H/D* = 2; and (b) *H/D* = 4

within the domain, there are two basic unknowns, namely, horizontal velocity (u) and vertical velocity (v). Along the boundaries CX and OX, it is specified that the values of the horizontal and vertical velocities become equal to zero; whereas along the boundary OQ and PY, the horizontal velocities become equal to zero. The periphery of the opening PQ is modeled as a stress free surface, that is, deformation can take place freely in any direction along this surface; hence, no velocity boundary constraints need to be imposed along this circular boundary.

4. Analysis

Following Sloan and Kleeman [18], an upper bound finite limit analysis has been performed by satisfying the kinematically admissible velocity field. Note that a kinematically velocity field is the one which satisfies compatibility, associated flow rule and the velocity boundary conditions. In addition, kinematically admissible velocity discontinuities are permitted along the interfaces of all the adjacent elements; that is, normal and tangential velocity jumps across any discontinuity line must satisfy the associated flow rule. The Mohr-Coulomb failure criterion is assumed to be valid. For plane strain conditions, the Mohr-Coulomb yield function (F) can be expressed as

$$F = \left(\sigma_x - \sigma_y\right)^2 + \left(2\tau_{xy}\right)^2 - \left(2c\cos\phi - \left(\sigma_x + \sigma_y\right)\sin\phi\right)^2 = 0 \tag{3}$$

To ensure that the finite-element formulation leads to a linear programming problem, it is necessary to express the yield criterion as a linear function of stresses. By following Bottero *et al.* [16], the Mohr-Coulomb yield criterion is linearized by drawing a symmetric arrangement of planes in a stress space. The linearized yield polygon is circumscribed to the parent yield circle so that the solution remains always a rigorous upper bound on the exact solution; Fig. 3 shows the linearized yield polygon for p = 3. For a polygon with p sides, the equation of the k^{th} side of the Mohr-Coulomb criterion becomes as

$$F_k = A_k\sigma_x + B_k\sigma_y + C_k\tau_{xy} - 2c\cos\phi = 0 \tag{4}$$

where $A_k = \cos a_k + \sin\phi$, $B_k = \sin\phi - \cos a_k$,

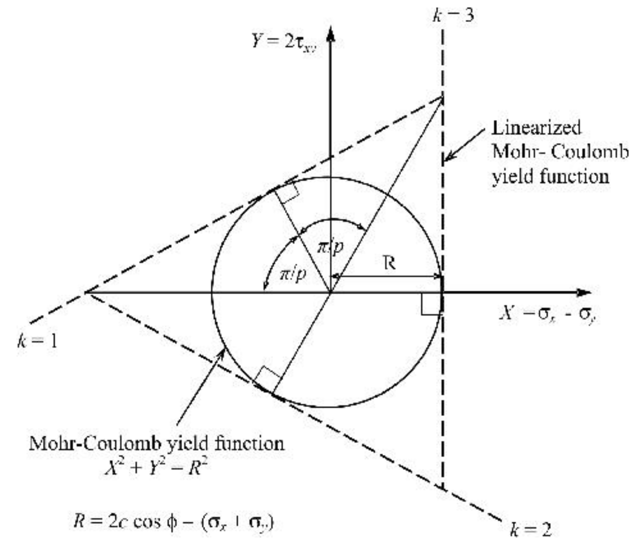

Fig. 3. The linearization of the Mohr-Coulomb yield criterion with p = 3

$C_k = 2\sin a_k$, $a_k = 2\beta k$, $\beta = \pi / p$, and k = 1, 2, …, p. Eq. (4) is associated with k^{th} side of the yield polygon joining the vertices k and (k+1) as shown in Fig. 3. The co-ordinates of these vertices in terms of the variables X and Y are given below:

$$\begin{aligned} X_k &= R\cos\left(a_k - \beta\right)/\cos\beta; \\ X_{k+1} &= R\cos\left(a_k + \beta\right)/\cos\beta; \end{aligned} \tag{5a}$$

$$\begin{aligned} Y_k &= R\sin\left(a_k - \beta\right)/\cos\beta; \\ Y_{k+1} &= R\sin\left(a_k + \beta\right)/\cos\beta; \end{aligned} \tag{5b}$$

where R is the radius of the yield circle drawn in the X-Y plane.

$$R = 2c\cos\phi - \left(\sigma_x + \sigma_y\right)\sin\phi \tag{5c}$$

The associated flow rule imposes three equality constraints on the nodal velocities and plastic multiplier rates for each element. For the linearized yield criterion defined by Eq. (4), the plastic strain rates are given by

$$\dot{\varepsilon}_x = \frac{\partial u}{\partial x} = \dot{\lambda}\frac{\partial F}{\partial \sigma_x} = \sum_{k=1}^{k=p}\dot{\lambda}_k\frac{\partial F_k}{\partial \sigma_x} = \sum_{k=1}^{k=p}\dot{\lambda}_k A_k \qquad \dot{\lambda}_k \geq 0 \tag{6a}$$

$$= \frac{\partial v}{\partial y} = \dot{\lambda}\frac{\partial F}{\partial \sigma_y} = \sum_{k=1}^{k=p}\dot{\lambda}_k\frac{\partial F_k}{\partial \sigma_y} = \sum_{k=1}^{k=p}\dot{\lambda}_k B_k \qquad \dot{\lambda}_k \geq 0 \tag{6b}$$

$$\dot{\gamma}_{xy} = \left(\frac{\partial v}{\partial x} + \frac{\partial u}{\partial y}\right) = \dot{\lambda}\frac{\partial F}{\partial \sigma_{xy}}$$

$$= \sum_{k=1}^{k=p} \dot{\lambda}_k \frac{\partial F_k}{\partial \tau_{xy}} = \sum_{k=1}^{k=p} \dot{\lambda}_k C_k \qquad \dot{\lambda}_k \geq 0 \tag{6c}$$

where $\dot{\lambda}_k$ = a non-negative plastic multiplier rate associated with the k^{th} side of the yield polygon; $\dot{\varepsilon}_x$ = plastic normal strain rate in x-direction; $\dot{\varepsilon}_y$ = plastic normal strain rate in y-direction; $\dot{\gamma}_{xy}$ = plastic shear strain rate; σ_x and σ_y are the normal stresses in x and y directions, respectively; and τ_{xy} is the shear stress. The parent yield circle is inscribed to the chosen linearized polygon so that the numerical solution always remains a rigorous upper bound on the exact solution. While performing the computations, the total numbers of sides of the yield polygon were taken equal to 24.

An upper bound on true collapse load can be obtained by minimizing the total power dissipated in the problem domain. The power dissipation occurs in the domain due to (i) presence of the velocity discontinuities and (ii) plastic straining of all the elements. For formulating the upper bound problem as a linear programming problem, the following equality constraint needs to be imposed:

$$\sum_{i=1}^{E} A_i\left(-v_i\right) = K \tag{7}$$

where (i) A_i is the area of the i^{th} element, (ii) v_i is the velocity in y direction at the centroid of the i^{th} element, (iii) E is the total number of elements in the domain, and (iv) K is a constant which needs to be always positive and provides the rate of the total external work done by the body forces $A_i\gamma$ in the vertical downward direction with a unit value of γ. Since v is taken as positive in the vertical upward direction, the negative sign has been assigned to v_i in Eq. (7).

The objective function along with the constraints in a kinematically admissible velocity field can be written in the following standard form so as to finally frame a linear programming problem:

Objective function: Minimize $\{C\}^T\{X\}$ (8)

Subject to constraints: $[A]\{X\} = \{B\}$ (9)

$\{C\} = \begin{Bmatrix} C_1 \\ C_2 \\ C_3 \end{Bmatrix}$ = global vector of the coefficients of the objective function

$$\{X\} = \begin{Bmatrix} X_1 \\ X_2 \\ X_3 \end{Bmatrix}$$

X_1 = global vector of the nodal velocities (unbounded)

X_2 = global vector of the element plastic multiplier rates (positive)

X_3 = global vector of the velocity discontinuity parameters (positive)

$[A]$ = Matrix of coefficients of the equality constraints

$\{B\}$ = global vector of constants on the right hand side of the constraints

For obtaining the solution of the problem, a computer code was written in MATLAB and the linear optimization was performed by using a subprogram '*linprog*' available in MATLAB for minimizing the objective function, the detailed computational procedure is elaborated in Kumar and Kouzer [21]. After minimizing the objective function, the value of maximum unit weight of soil (γ_{max}) is determined by using the following expression:

$$\gamma_{\max} = \frac{Min\{C\}^T\{X\}}{K} \tag{10}$$

It should be mentioned that the value of γ_{max} remains always independent with respect to any chosen positive value of K. By knowing the value of γ_{max}, the value of the stability number (S_n) is then computed by using Eq. (2).

5. Results and Comparisons

5.1. The Variation of the Stability Number (S_n)

The variation of the stability number S_n with changes in *H/D* has been obtained for different values of *m*. In order to obtain the computational results (i) the value of *H/D* was varied from 1 to 7, and (iii) six different magnitudes of *m*, namely, 0, 1, 2, 3, 4 and 5, were chosen. The computational results are presented in Fig. 4 and Table 1. It can be seen that the magnitude of the stability number increases continuously with an increment in the values of both *H/D* and *m*.

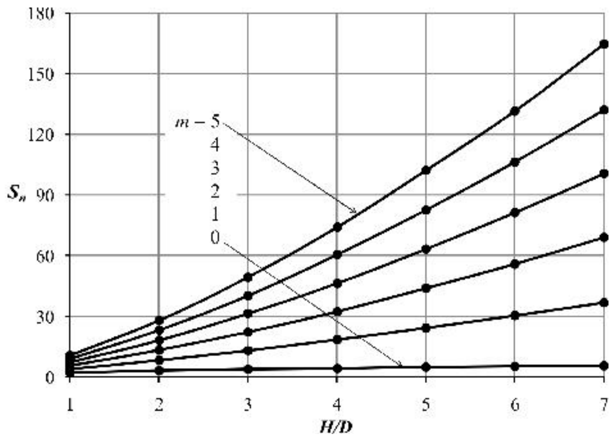

Fig. 4. The variation of S_n with *H/D* for different values of *m*

The results obtained from the present analysis imply that for a given *H/D*, the maximum height which can be permitted by a circular opening of diameter *D* increases with an increase in values of *m*. On the other hand, the maximum height which the opening can permit, will increase with an increase in *H/D* (or in other words with a reduction in the diameter of the tunnel for a given H). It should be mentioned that from the basic definition of the stability number, it can be easily concluded that the maximum permissible height for a given diameter of the tunnel will increase continuously with (i) an increase in soil cohesion and (ii) a decrease in the unit weight of soil mass.

Table 1. The values of S_n for different combination of *H/D* and *m*

H/D	*m*					
	0	1	2	3	4	5
1	2.05	3.93	5.67	7.39	9.09	10.78
2	3.07	8.26	13.24	18.18	23.11	28.04
3	3.76	13.12	22.20	31.24	40.28	49.30
4	4.34	18.52	32.41	46.27	60.54	74.24
5	4.81	24.31	43.85	63.21	82.75	102.12
6	5.22	30.25	55.93	81.31	106.17	131.38
7	5.51	36.75	69.01	100.43	132.20	164.78

For the purpose of comparison, the values of S_n obtained from the present study for $m = 0$ were compared with (ii) the upper bound solution of Osman *et al.* [6] on the basis of an assumed collapse mechanism, and (ii) the numerical upper bound limit analysis solution given by Yamamoto *et al.* [8] based on nonlinear programming. The comparison of these results are provided in Fig. 5; note that the existing results of Osman *et al.* [6] and Yamamoto *et al.* [8] have been reported only up to $H/D = 5$ and, moreover, these results are available only for $m = 0$. It can be noted that in all the cases the results from the present analysis are marginally lower than the results of Osman *et al.* [6] and compare quite closely with the available solutions of Yamamoto *et al.* [8].

5.2. Nodal Velocity Patterns

Nodal velocity patterns were examined for $H/D = 2$ and 4 with two different values of *m*, namely, 0 and 5. These nodal velocity patterns are illustrated in Figs. 6 and 7. The arrow line drawn at any point represents the magnitude and direction of the resultant velocity. If there are two or more straight lines at the same point, it implies the presence of the line of velocity discontinuity in the domain. The nodal velocities have been found to be always in vertical downward direction

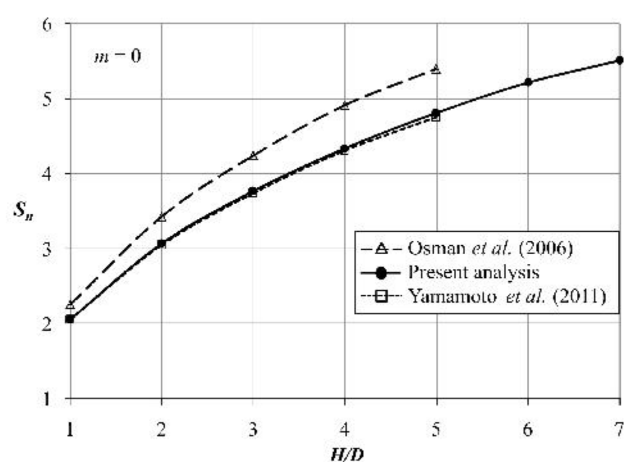

Fig. 5. A comparison of the present results with those available in literature

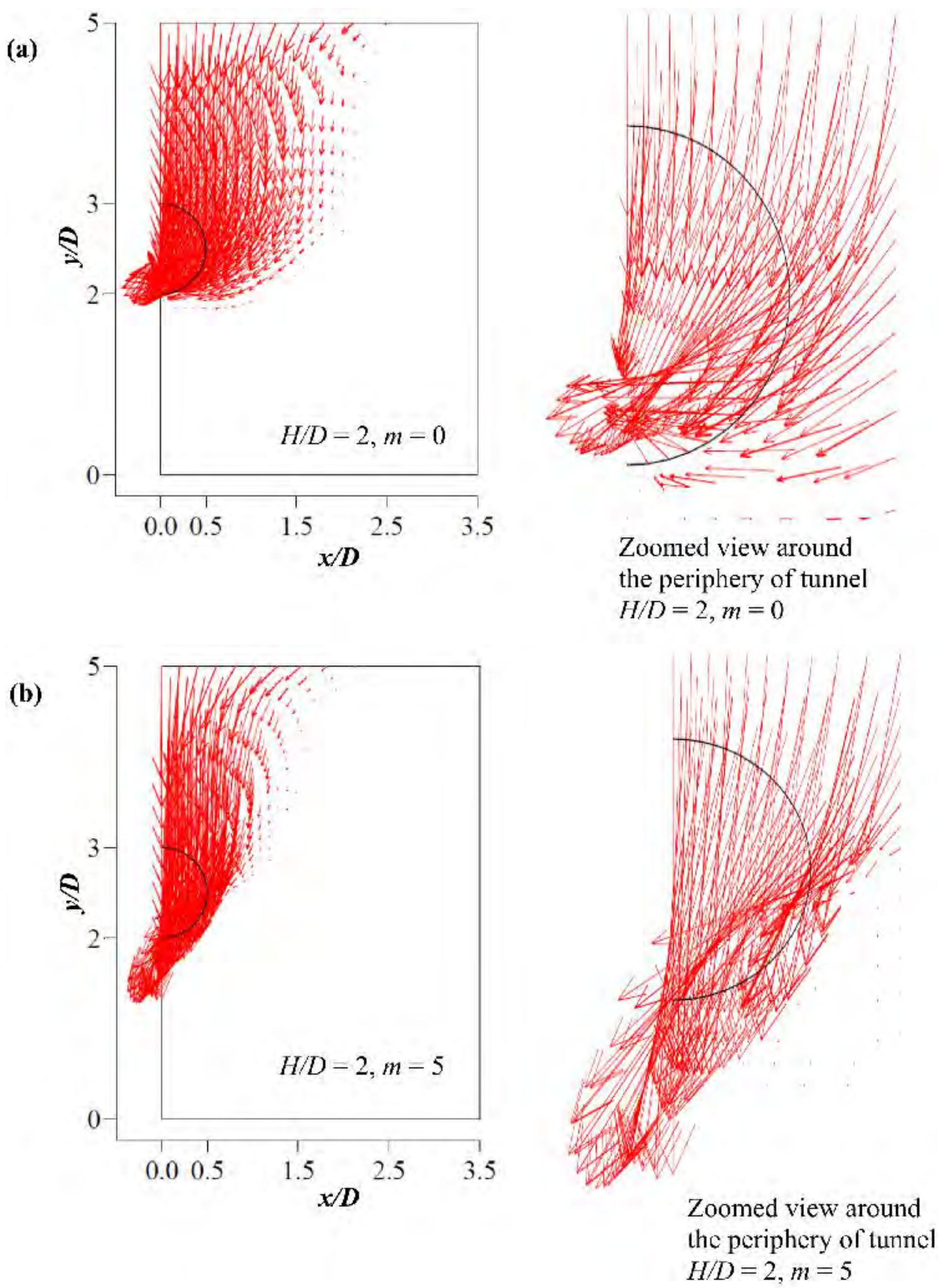

Fig. 6. The variation of nodal velocity patterns for *H/D* = 2 with (a) *m* = 0; and (b) *m* = 5

at the crest of the tunnel. On the other hand, at the bottom of the tunnel (i) for $m = 5$, hardly any movement of the soil has been observed and (ii) for $m = 0$, a considerable vertical upward movement (heave) of the soil is noted. The nodal velocities around the perimeter of the tunnel for $m = 5$ are found to be generally much greater as compared to those obtained with $m = 0$. The boundary of the rupture zone in all the cases has been found to become curvilinear; the rupture zone refers to a region in which the magnitudes of the nodal velocities were found to be significant. Note that the size of the failure zone becomes consistently smaller for lower values of H/D and greater values of m.

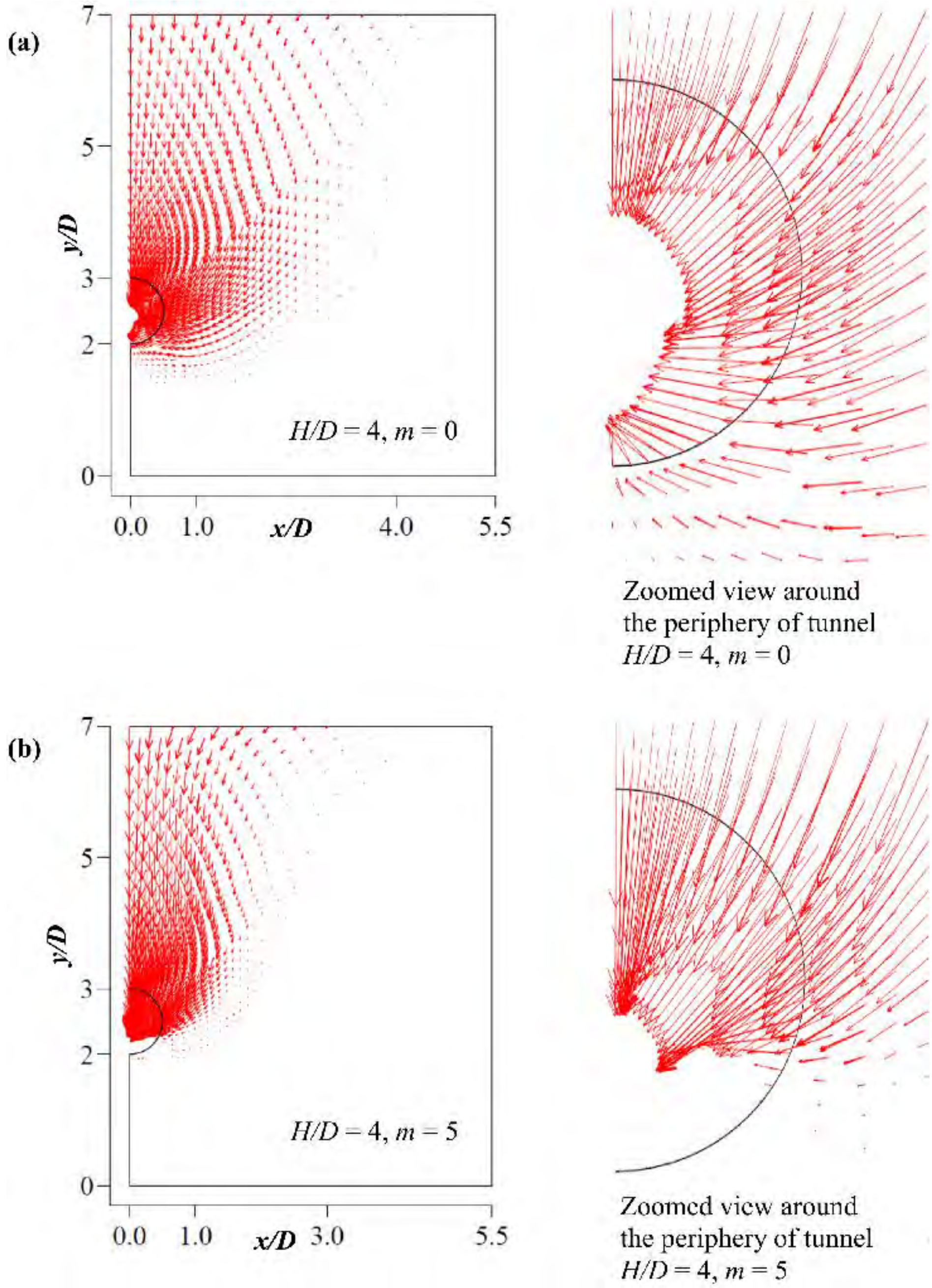

Fig. 7. The variation of nodal velocity patterns for *H/D* = 4 with (a) *m* = 0; and (b) *m* = 5

Conclusions

The stability of a long unsupported circular tunnel (opening) formed in a clayey soil medium has been determined by employing the upper bound limit analysis in combination with finite elements and linear programming. The stability of the tunnel has been assessed with the help of a non-dimensional stability number, the variation of which has been established as a function of m and H/D. With an increase in the values of H/D and m, the stability numbers increase continuously. The size of the failure zone increases continuously (i) with an increase in the values of H/D, and (ii) with a decrease in the values of m. The numerical results presented in this paper are found to compare well with that available in literature for $m = 0$.

References

1 J H Atkinson and D M Potts *Geotechnique* **27** (1977)

2 E H Davis, M J Gunn, R J Mair and H N Seneviratne *Geotechnique* **30** (1980)

3 E Leca and L Dormieux *Geotechnique* **40** (1990)

4 S W Sloan and A Assadi *Comput Geotech* **12** (1991)

5 B R Wu and C J Lee *Int J Phys Model Geotech* **4** (2003)

6 A S Osman, R J Mair and M D Bolton *Geotechnique* **56** (2006)

7 F Yang and J S Yang *Int J Geomech ASCE* **10** (2010)

8 K Yamamoto, A V Lyamin, D W Wilson, S W Sloan and A J Abbo *Comput Geotech* **38** (2011)

9 K Yamamoto, A V Lyamin, D W Wilson, S W Sloan and A J Abbo *Can Geotech J* **48** (2011)

10 W F Chen *Limit Analysis and Soil Plasticity* Elsevier Amsterdam (1975)

11 E J Murray and J D Geddes *Geotechnique* **39** (1989)

12 W F Chen and X L Chen *Limit Analysis in Soil Mechanics* Elsevier Amsterdam (1990)

13 R L Michalowski *Soils Found* **37** (1997)

14 A H Soubra *Can Geotech J* **37** (2000)

15 J Kumar *Can Geotech J* **39** (2002)

16 A Bottero, R Negre, J Pastor and S Turgeman *Comput Methods Appl Mech Engng* **22** (1980)

17 S W Sloan *Int J Numer Analyt Meth Geomech* **13** (1989)

18 S W Sloan and P W Kleeman *Comput Methods Appl Mech Engrg* **127** (1995)

19 B Ukritchon, A W Whittle and C Klangvijit *J Geotech Geoenviron Engng ASCE* **129** (2003)

20 A W Bishop *Geotechnique* **16** (1966)

21 J Kumar and K M Kouzer *J Geotech Geoenviron Engng ASCE* **133** (2007).